Biodynamic Pilot Modelling for Aero-Elastic Aircraft

L.Zaichik, Y.Yashin, P.Desyatnik and H.Smaili***
**Central Aerohydrodynamic Institute (TsAGI), Zhukovsky, Russia*
zaichik@tsagi.ru
***National Aerospace Laboratory (NLR), Amsterdam, the Netherlands*
hafid.smaili@nlr.nl

Abstract
Results are presented received in the course of project ARISTOTEL of the 7th European Framework Program (http://www.aristotel.progressima.eu/), which studies adverse interaction between pilots and aircraft. The present paper considers effects of control inceptor type and feel system characteristics on the biodynamical interaction in presence of disturbing high-frequency lateral accelerations. The analysis is performed which allows splitting the pilot activity into "active" component (active pilot) and "passive" component (biodynamical pilot). Received experimental database allowed identification of transfer functions of the pilot models and the rules of their parameter adjustment as functions of control inceptor type and feel system characteristics. In perspective, the results will be used to develop criteria to assess the effect of structural elasticity on aircraft handling qualities.

1. Introduction

Figure 1 shows block-diagram of the operational activity of a pilot, who performs deliberate control actions. The pilot-aircraft loop is closed by visual and motion (acceleration) feedbacks. According to the categories given in [1,2], accelerations are known to affect piloting beneficially in some cases and negatively in some others: on the one hand, accelerations are the information factor, that is they give the information of aircraft motion which helps a pilot to control an aircraft; on the other hand, accelerations are the physiological (biodynamical) factor as they cause body displacement which may be assessed negatively by the pilot.
The high-frequency oscillations due to structural elasticity refer to the biodynamic factor, since they lead to involuntary body and limb-manipulator system displacements, which interfere with pilot voluntary control activity and, finally, worsen handling quality ratings.

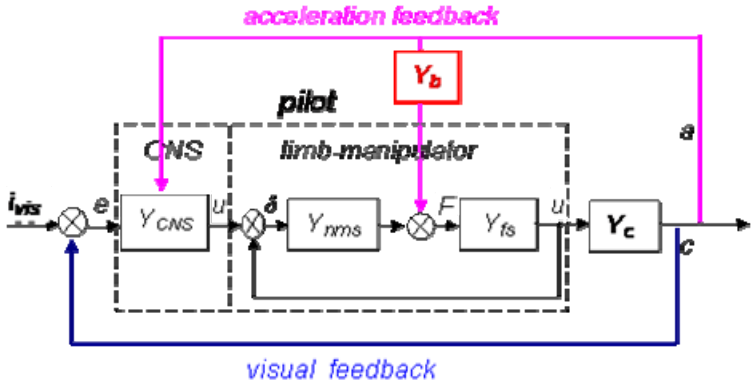

Figure 1: Block-diagram of the pilot-aircraft model with visual and motion feedbacks

When a pilot controls an elastic aircraft, he, on the one hand, performs a piloting task, and, on the other hand, he is exposed to the disturbing high-frequency oscillations due to structural elasticity. In other words, pilot control activity consists of two components: deliberate and involuntary, created by so-called "active" and "biodynamical" pilots. The two "pilots" are differently motivated since their inputs are different: for "active" pilot, the input is a visual signal; for "biodynamical" pilot, the input is the high-frequency oscillations. The characteristic frequency ranges of the pilot

models are also different: the “active pilot” is limited in the region 1.0-1.5 Hz; the “biodynamical” pilot is above 1.5 Hz. These facts allow us to consider the “active” and “biodynamical” pilot models separately.
Existing aircraft-pilot coupling (APC) criteria do not practically take into account manipulator feel system characteristics, although the control inceptor, being a part of pilot-aircraft model, and its characteristics can affect the “active” and “biodynamical” components of the pilot control activity. Taking into account the reasoning above, the effect of manipulator feel system characteristics are considered for the “active” and “biodynamical” pilot models separately.

2. Database for the Model Development

The database for the pilot models development were experimental describing functions determined from “biodynamical” experiments. Experiments were conducted in flight simulators of TsAGI (PSPK-102) and NLR (GRACE) (Figure 2).

Figure 2: TsAGI PSPK-102 (left) and NLR GRACE (right) research flight simulators used in the experiment

2.1 Setup of experiments

Two series of experiments were conducted to determine biodynamic interaction characteristics: (1) without piloting and (2) with piloting. Below the description of experiments is given.
Experiment #1: Without pilot-in-the-loop
The diagram of the experimental setup without pilot-in-the-loop is shown in Figure 3.

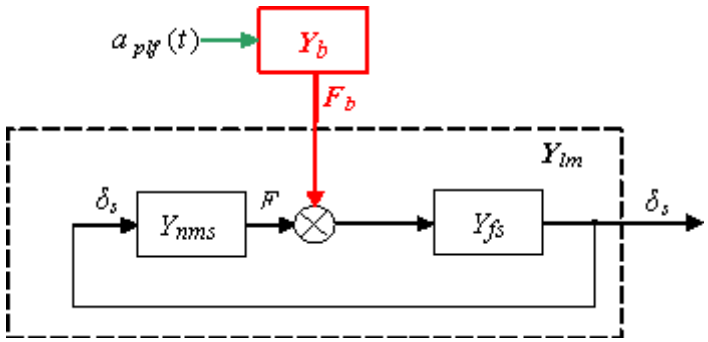

Figure 3: Biodynamic experiment setup without pilot-in-the-loop

The pilot (operator) had to hold the manipulator in a certain deflected position, controlling the position visually (the position of the manipulator was displayed).

The motion platform was moved in accordance with the following input signal:

$$a_{plf}(t) = \sum_{m=1}^{17} A_m \sin(\omega_m t + \varphi_m) . \quad \textbf{(1)}$$

Parameters to vary were:
- manipulator types (sidestick, wheel);
- feel system characteristics (force gradient F_{δ_s}, damping $F_{\dot{\delta}_s}$, friction F_{fr}, breakout force F_{br})

Recorded parameters were acceleration sensors outputs, manipulator position and manipulator force transducer output.

As a result of the experiments, the describing functions of the biodynamic interaction δ_s / a were received. The describing functions were determined through cross and auto spectral density, which were calculated using fast Fourier transform (FFT):

$$\left\{\frac{\delta_s}{a}\right\}(j\omega) = \frac{S_{a-\delta_s}(j\omega)}{S_{a-a}(j\omega)} , \quad \textbf{(2)}$$

where δ_s is stick displacement; a is accelerations produced by motion platform.

The time of each run was 50.96 sec. The frequency of signals recording was 100 Hz. The numbers of points considered were 4096 (first 10 sec were excluded because of the pilot (operator) adapted to the task).

Experiment #2: With pilot-in-the-loop

The diagram of the experimental setup with pilot-in-the-loop is shown in Figure 4.

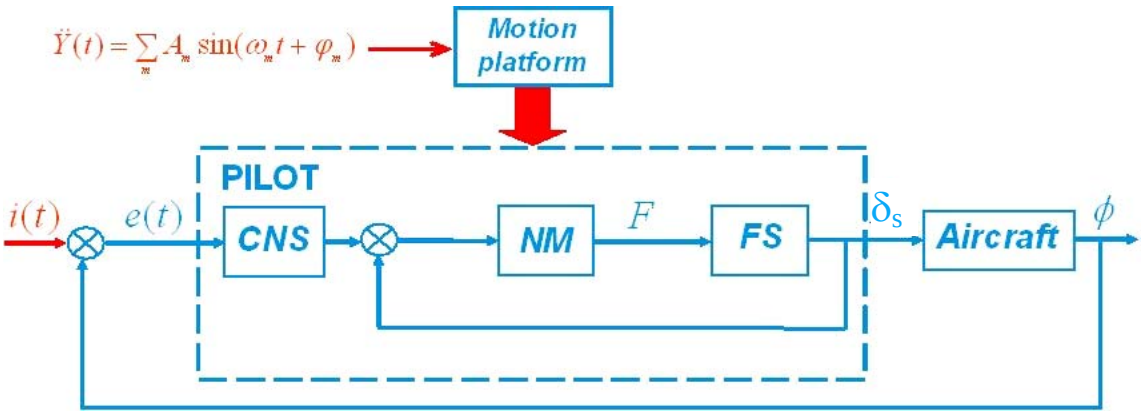

Figure 4: Biodynamic experiment setup with pilot-in-the-loop

In accordance with Figure 4, two uncorrelated disturbing factors (stimulus) were acting on the pilot during the experiment:

- Visual input signal in roll $i(t) = \sum_i A_i \sin(\omega_i t + \varphi_i)$, where $i = 1...17$;
- Lateral acceleration forcing function $\ddot{Y}(t) = \sum_m A_m \sin(\omega_m t + \varphi_m)$, where $m = 1...17$.

The pilot performed the tracking task as tight as possible under the action of lateral acceleration.

Parameters to vary were:
- manipulator types (sidestick, wheel);
- feel system characteristics (force gradient F_{δ_s}, damping $F_{\dot{\delta}_s}$, friction F_{fr}, breakout force F_{br}).

Recorded parameters were acceleration sensors outputs, visual input signal ($i(t)$), manipulator position signal δ_s, aircraft bank angle (ϕ), tracking error ($e(t)$).

As a result of the experiments, the describing functions of the active pilot δ_s / i were received. The describing functions were determined through cross and auto spectral density, which were calculated using fast Fourier transform (FFT):

$$\left\{\frac{\delta_s}{e}\right\} = \frac{S_{\delta_s - \phi}(j\omega)}{S_{e-\phi}(j\omega)}, \tag{3}$$

where δ_s is stick displacement; e is a visual tracking error signal; ϕ is aircraft bank angle.

The time of each run was 50.96 seconds. The frequency of the signals recording was 100 Hz. The numbers of points considered were 4096 (first 10 sec were excluded because of the pilot (operator) adaptation to the task).

Two NLR pilots, two TsAGI pilots and two TsAGI human-operators participated in experiments. All of the pilots have a vast experience on the hexapod simulators for different piloting tasks. As a whole, more than 650 runs were performed with the subjects.

All the inceptors were loaded by the electrical loading system, which allows flexible changing of feel system characteristics. The manipulator forces were modeled in accordance with the following equation:

$$m\ddot{\delta}_s + F_{\dot{\delta}_s}\dot{\delta}_s + F_{\delta_s}\delta_s = F_{br}\,\mathrm{sgn}\delta_s + F_{fr}\,\mathrm{sgn}\dot{\delta}_s + F_p, \tag{4}$$

where: m is inceptor mass, $F_{\dot{\delta}_s}$ is damping, F_{δ_s} is force gradient, F_{br} is breakout force, F_{fr} is friction, F_p is pilot force.

Some of the results of the biodynamical tests are presented in [3]. Here, we give more thorough analysis of the completed experimental data. The experimental describing functions are presented in Figures 5 – 7 for the active pilot model, and in Figures 8 – 10 for the biodynamical pilot model.

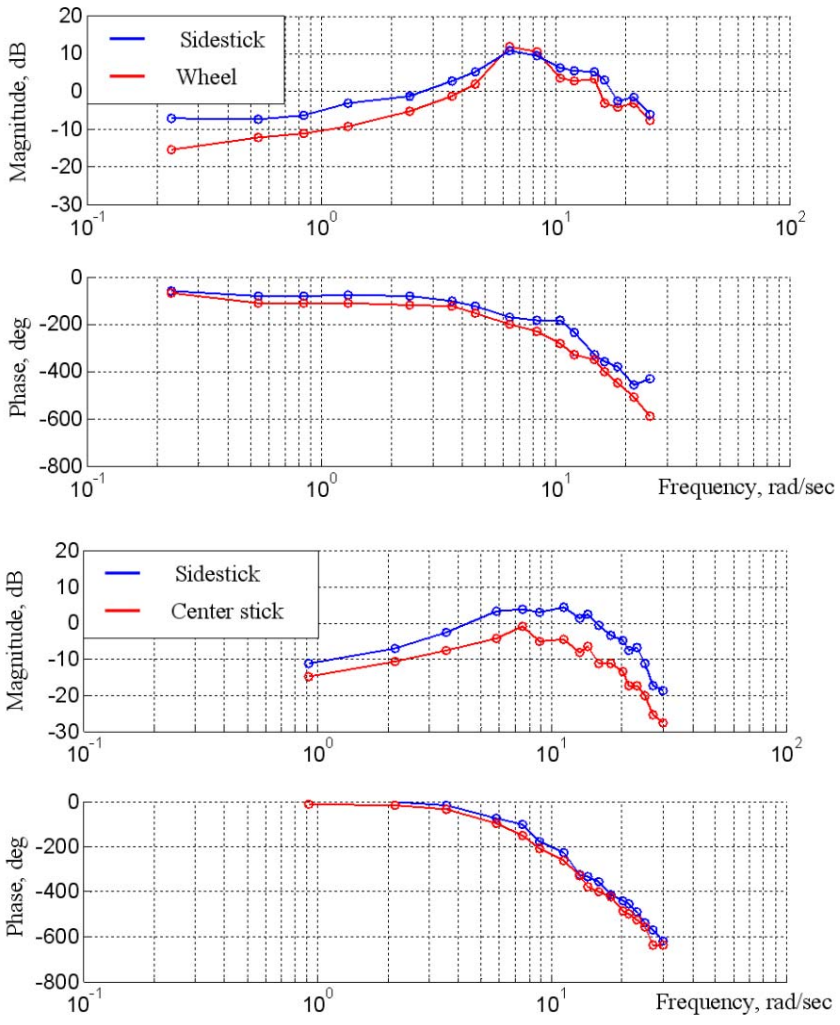

Figure 5: Active pilot. Effect of inceptor type. TsAGI data (upper) and NLR data (lower)

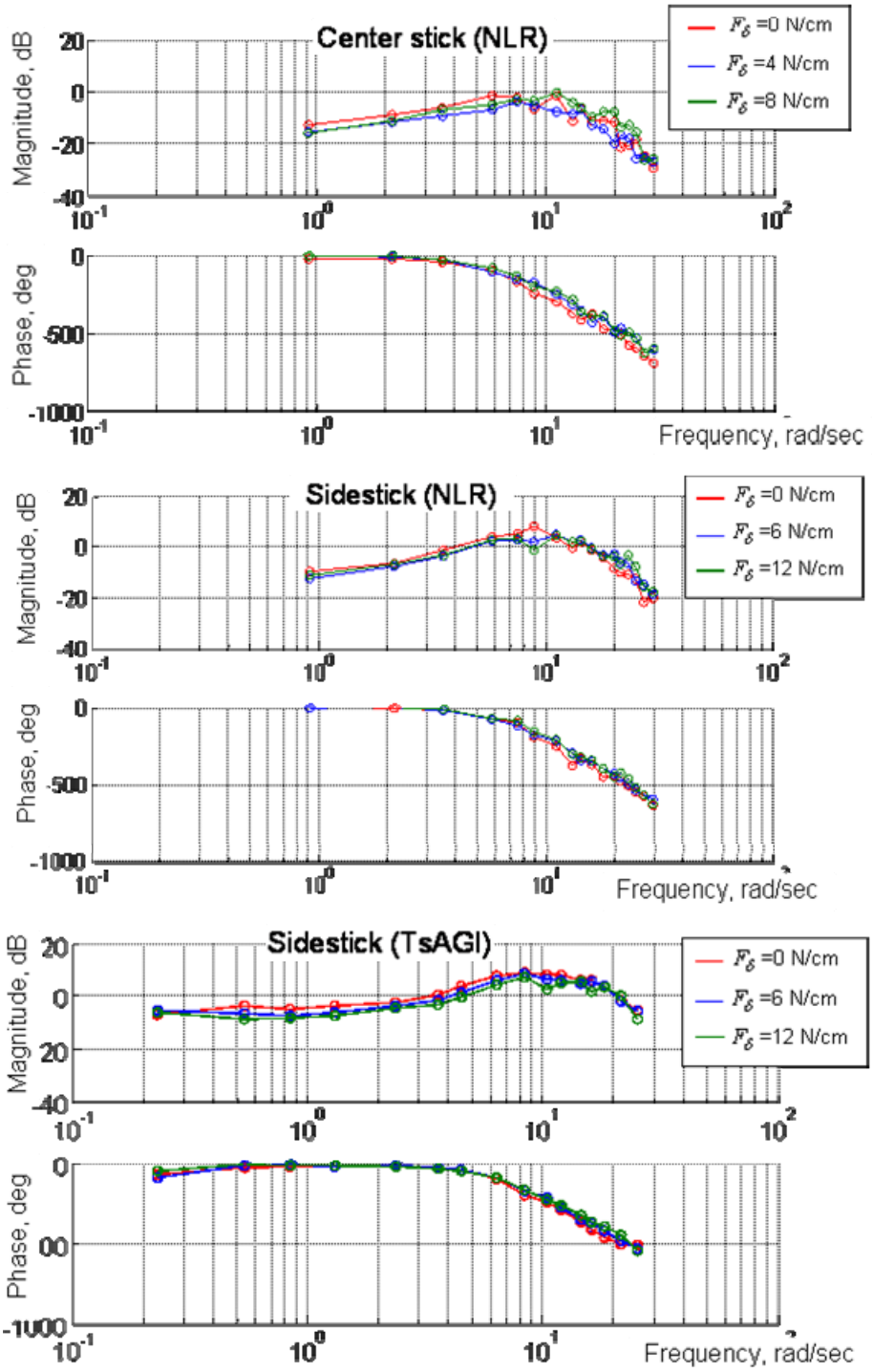

Figure 6: Active pilot. Effect of force gradient for center stick and sidestick

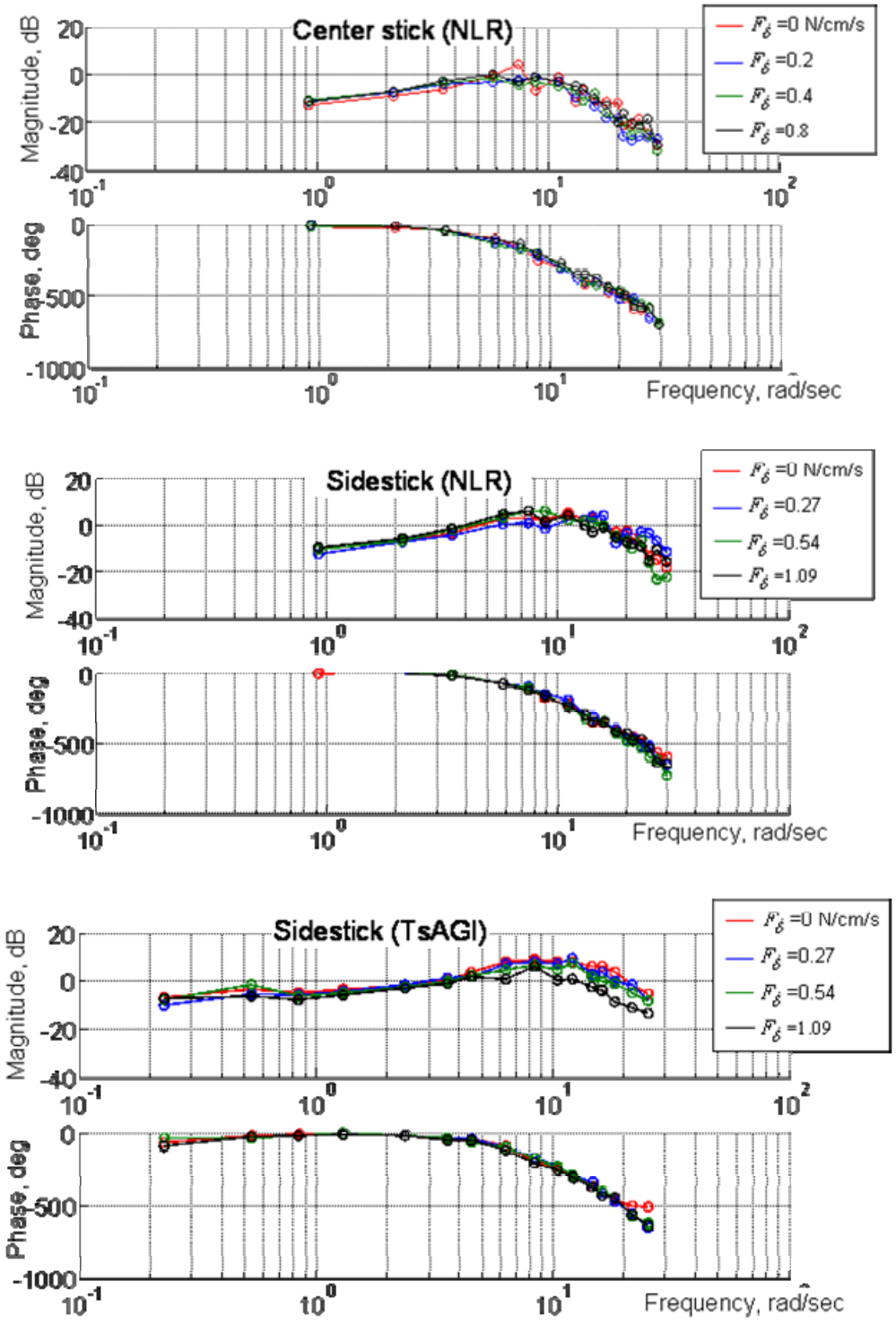

Figure 7: Active pilot. Effect of damping for center stick and sidestick

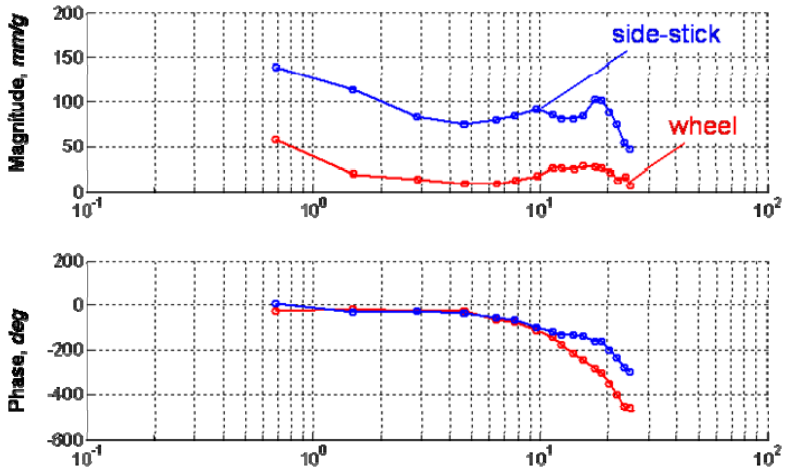

Figure 8 : Biodynamical pilot. Effect of inceptor type. (TsAGI PSPK-102)

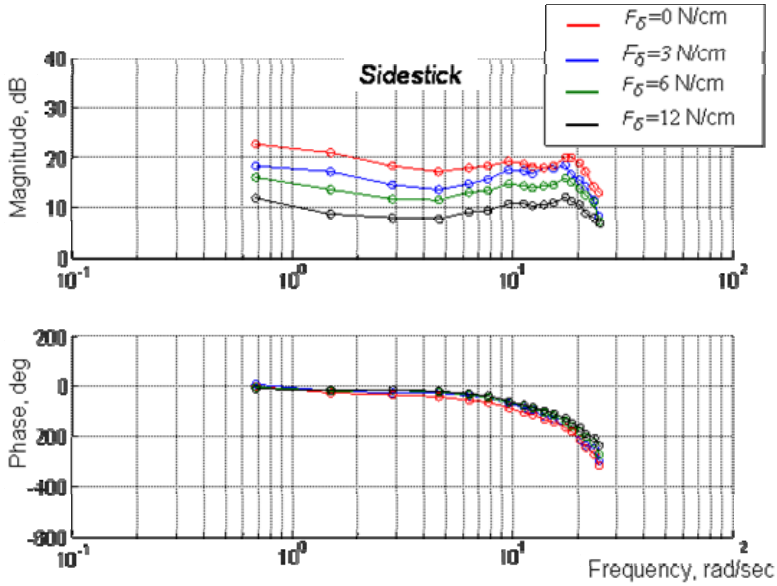

Figure 9: Biodynamical pilot. Effect of sidestick force gradient. (TsAGI PSPK-102)

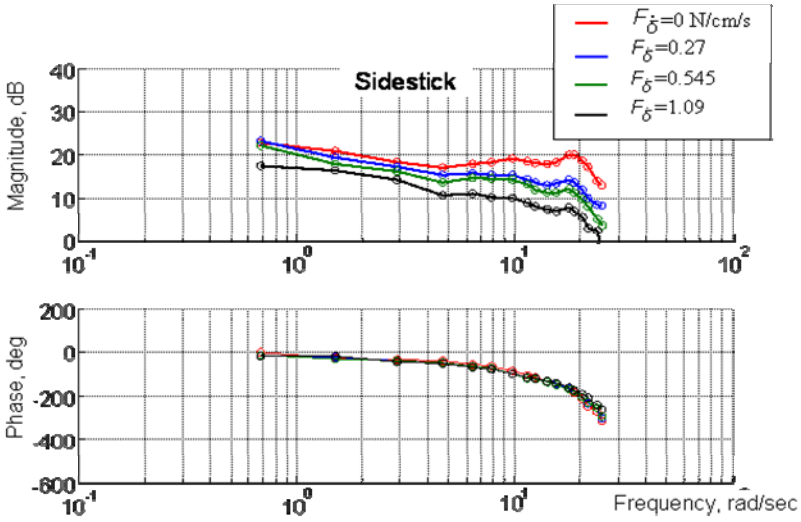

Figure 10: Biodynamical pilot. Effect of sidestick damping. (TsAGI PSPK-102)

2.2 Analysis of experimental data

Before we start analysis of the experimental data, a few general observations should be made:
1. Effect of inceptor feel system characteristics on pilot describing functions do not practically depends on pilots' inertial characteristics (size and weight), at least for the sidestick and wheel control. For the sidestick, it can be attributed to the arm resting on the armrest; for the wheel it is attributed to the fact the wheel displacements created by one hand are compensated for by that created by the other hand. This fact allows us to average the data received for all pilots, and make general conclusions. Nevertheless, for a central stick the effect of pilots' inertial characteristics may be more evident due to the lack of the armrest in this case.
2. Effect of feel system characteristics on, accordingly, active and biodynamic pilot models can be analyzed for the frequency ranges typical of the models. For active pilot model it is frequencies below 1.5 Hz; for biodynamical pilot model it is frequencies above 1.5 Hz.
3. As it was stated in previous publications (see, for example, [3]), within a limited range of friction and breakout forces variation, the effect of breakout force on biodynamic interaction (BDI) is somewhat similar to the effect of force gradient, and the effect of friction is similar to the effect of damping. Thus, we will pay here the greater attention to the effect of force gradient and damping.
The effects of inceptor type and feel system characteristics are considered separately for active pilot and for biodynamic pilot.

2.2.1 Active pilot data

1) The inceptor type affects the describing function gain at the low frequencies. Figure 5 presents data received for the wheel, central and side sticks for the close-to-optimum values of their feel system characteristics (wheel: F_{δ_s} =2 N/cm, $F_{\dot{\delta}_s}$ =0.27 N/cm/s, F_{br} =0, F_{fr} =0; side stick: F_{δ_s} = 6 N/cm, $F_{\dot{\delta}_s}$ =0.27 N/cm/s, F_{br} =0, F_{fr} =0; central stick: F_{δ_s} =8 N/cm, $F_{\dot{\delta}_s}$ =0, F_{br} =0, F_{fr} =0). The data were received on TsAGI's PSPK-102 flight simulator (wheel and sidestick) and NLR GRACE flight simulator (center stick and sidestick). Compared to traditional inceptors (wheel and central stick) a sidestick has 2.5 – 3 times less displacements, higher velocity capabilities, lower time delay. In other words, the limb-manipulator system with a sidestick has higher dynamic properties.
This conclusion is supported by experiments. Figure 11 presents data received earlier in [4]. It is seen that for a sidestick the pilot delay τ decreases compared to the traditional wheel and center stick. As a result, the overall pilot response time decreases, and pilot gain increases. The data were received for the pitch axis, but, in kind, they can be applied to the roll control axis as well. Thus, it is natural that the active pilot describing function for a sidestick has greater gain than that for the wheel and center stick.
2) If inceptor force gradient is within the range typical of practice (for a sidestick it is within 3-6 N/cm), its variation does not affect active pilot describing function (Figure 6). The effect of gradient is not noticeable outside the optimum range as well, though some tendencies can be detected. As forces gradient is smaller than optimum or zero, the inceptor deflections become more extensive, and the describing function gain increases at the low frequencies. As the force gradient increases over the optimum, the gain slightly decreases due to the reduced capabilities of neuromuscular system to adapt to increased inceptor forces.
Usually, the force gradient is selected from point-of-view of the rigid-body aircraft handling qualities; its optimum values vary in the rather narrow range. As force gradient deflects from the optimum values, the pilot ratings deteriorate: due to (low-frequency) PIO tendency for values smaller than optimum; due to too large inceptor forces for gradient values greater than optimum. The pilot ratings deterioration can be estimated in accordance with the function presented in Figure 12 [5].
It should be mentioned also that the subjective pilot ratings appeared to be more "sensitive" to force gradient variation than the pilot describing function.
The data received at TsAGI and NLR for sidestick are comparable in terms of the effect of feel system characteristics, but different in terms of gain. This difference is natural, since the experiments were conducted in different simulators, different visual inputs (their spectrum were different) and different aircraft command gradients (gains) were used. These factors may affect the active pilot gain, i.e. amplitude of frequency response.
3) Figure 7 shows that the inceptor damping does not affect active pilot describing function at the low frequencies for the rather wide range of the parameter variation (from 0 up to very large damping, which is unusual for practice). The point is that at the frequencies typical of active control, the introduction of additional damping does not lead to any noticeable increase of inceptor forces felt by a pilot, and, thus, does not affect handling qualities pilot ratings.
To confirm the statement, Figures 13, 14 shows the data received for the wheel in the course of one of TsAGI study. Figure 13 shows pilot ratings received for the two test pilots for different values of the damping coefficient; the

values varied from ζ=0.3 up to 1.2. It is seen that despite of the fact the damping varied in a large range, the pilot ratings do not noticeably changed. Figure 14 shows the percentage of forces due to damping referred to the total wheel forces estimations as a function of force gradient and damping coefficient. It is seen, in particular, that the greater is force gradient, the smaller is the contribution of damping forces.
At high frequencies above 1.5-2 Hz, there is a certain drop in describing function amplitude, which increases with damping. But such describing function distortions are the matter of biodynamical pilot component rather than active pilot.

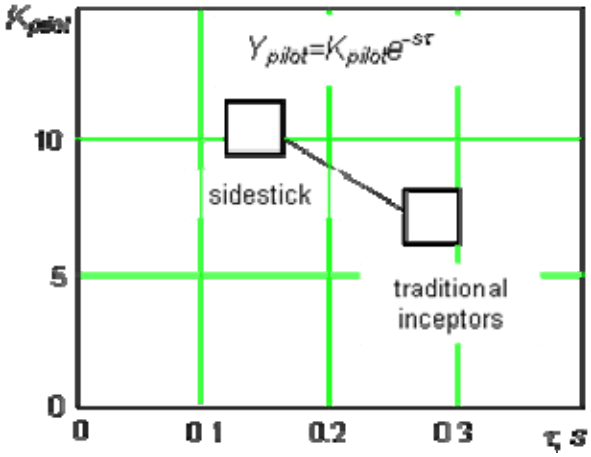

Figure 11: Dynamic properties of an active pilot in pitch with different inceptors

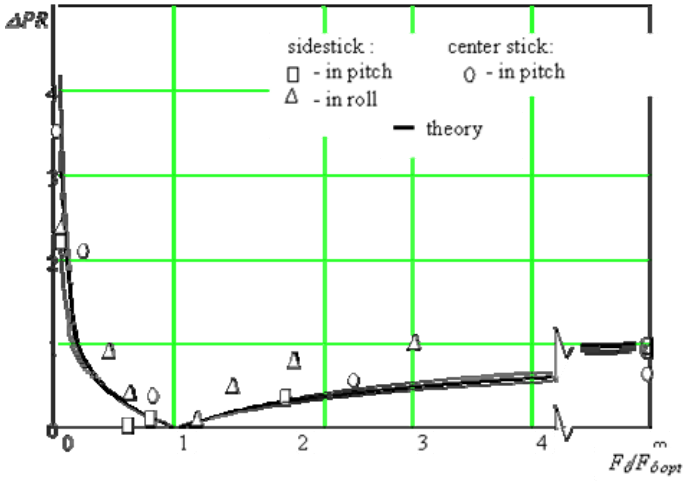

Figure 12: Pilot ratings of the rigid-body aircraft vs inceptor force gradient

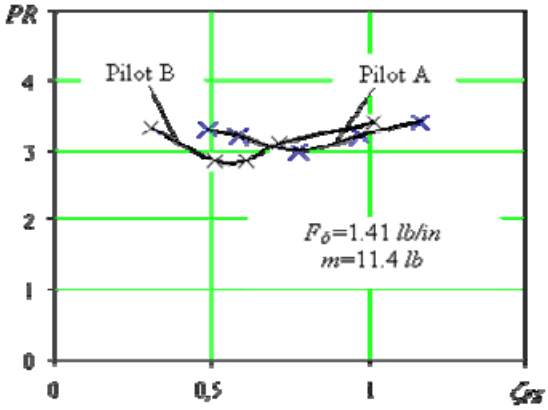

Figure 13: Pilot ratings as a function of wheel damping ratio

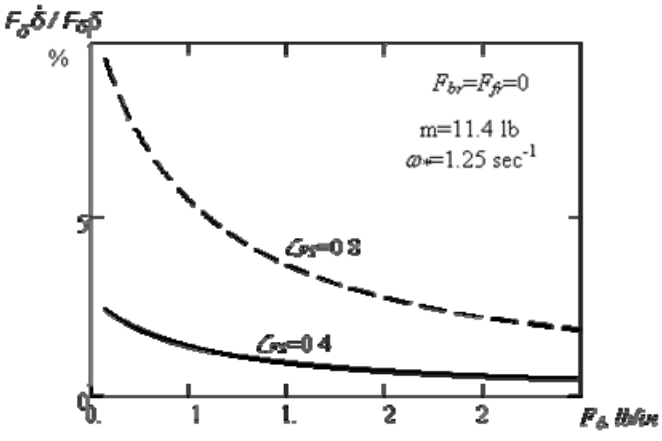

Figure 14: The contribution of the damping force to the total wheel force

2.2.2 Biodynamical pilot data

1) The type of inceptor affects biodynamical interaction (BDI) intensity in a considerable extent. Figure 8 shows that, in degree, BDI tendency with a wheel 3 times less than with a sidestick. In kind, the effect of feel system characteristics on BDI is similar for the wheel and sidestick. Therefore, the further analysis of the feel system effect will be conducted based on sidestick results.
2) As it is seen from Figure 9, if the force gradient is within its optimum range, its variation does not noticeably reduce BDI tendency within the whole range of frequencies. To make the reduction of BDI tendency more effective, we need to increase the force gradient more than twice as much. But this can lead to handling quality ratings worsening (see Figure 12).
3) As inceptor damping increase, the BDI tendency decreases noticeably, at high frequencies in particular: as $F_{\dot{\delta}_s}$ increases from 0.25 to 1.0 N/cm/s, the high-frequency oscillations tendency becomes 4 times less (Figure 10). It should be mentioned that within the values considered in experiments, the effect of damping on pilot ratings is practically negligible (see Figures 13, 14).
Thus, the analysis conducted allows us to make a few conclusions useful for pilot modeling:
1. Inceptor feel system characteristics do not practically affect describing function of the active pilot, though can worsen considerably pilot ratings of aircraft handling qualities.
2. Biodynamical interaction (biodynamical pilot describing function) depends on the type of inceptor. Among the traditional wheel and a sidestick, the BDI is less pronounced for the wheel.
3. Inceptor damping is the most effective method to suppress high-frequency oscillations, since, first, its variation in a wide range does not worsen pilot HQ ratings, and, second, it decreases the high-frequency inceptor oscillations in a considerable extent.

3. Pilot Modelling to Take Into Account Inceptor Feel System Characteristics

The analysis performed in the previous Chapters allows identification of the pilot model transfer functions. In accordance with the assumed splitting of the pilot activity, transfer functions are identified for the “active” and “biodynamical” pilot models.
The modern mathematical software, such as Matlab and others, allows identification of a system transfer function on the basis of its frequency response. The transfer function received in such a way is the function, which numerator and denominator are high-order polynomials. But in this case, any other feel system configuration is described by new polynomials with new set of coefficients, and no adjusting rules can be determined for these coefficients as a function of feel system characteristics. Thus, the transfer functions identified by polynomials can not be applied for further study of the effect of feel system characteristics and for the development of HQ criteria. The adjustment rules can be determined if the structure of the transfer function is known and given as a set of elementary functions (aperiodic, oscillatory, etc.). The main goal of the present Chapter is to determine the structure of transfer functions for the active and biodynamical pilot models, and to determine the rules of their parameters adjustment as a function of feel system characteristics.

3.1 Active pilot modelling

The describing functions of active pilot model (visual tracking) presented in Figures 5 – 7 show that there are two resonant peaks in amplitude characteristics at the frequencies above 1 Hz. This is characteristic of the function of no less than the fourth order. The comparison of the experimental describing functions and that calculated in accordance with the identified transfer functions, which is conducted later on, shows that the best coincidence of the describing functions is achieved for the transfer function of the following structure:

$$\mathrm{Y_{ap}}(s) = K \cdot e^{-s\tau} \cdot (T_L s + 1) \cdot \left[\frac{1}{T_1^2 s^2 + 2T_1 \zeta_1 s + 1} \right] \cdot \left[\frac{1}{T_2^2 s^2 + 2T_2 \zeta_2 s + 1} \right]. \qquad \textbf{(5)}$$

The active pilot model (5) differs from the generally used model by the two additional oscillatory units, which describe the limb-manipulator system dynamics.
The analysis conducted above shows that the feel system characteristics do not practically affect active pilot describing function. Thus, from point of view of the best coincidence of the experimental and calculation data, we

can propose the following values for the parameters of function (1) regardless of feel system characteristics and the type of inceptor:

τ=0.2s; T_L=0.4s; T_1=0.12s; ζ_1=0.3s; T_2=0.05s; ζ_2=0.3s.

It should be mentioned that the identified values of τ and T_L are typical of that generally used to describe pilot control behavior.

The values of gain coefficient K in (5) are functions of the type of inceptor and aircraft control sensitivity.

Figure 15 confirms the validity of the identified transfer functions by their comparison with the experimental describing functions of the active pilot model for different inceptor types.

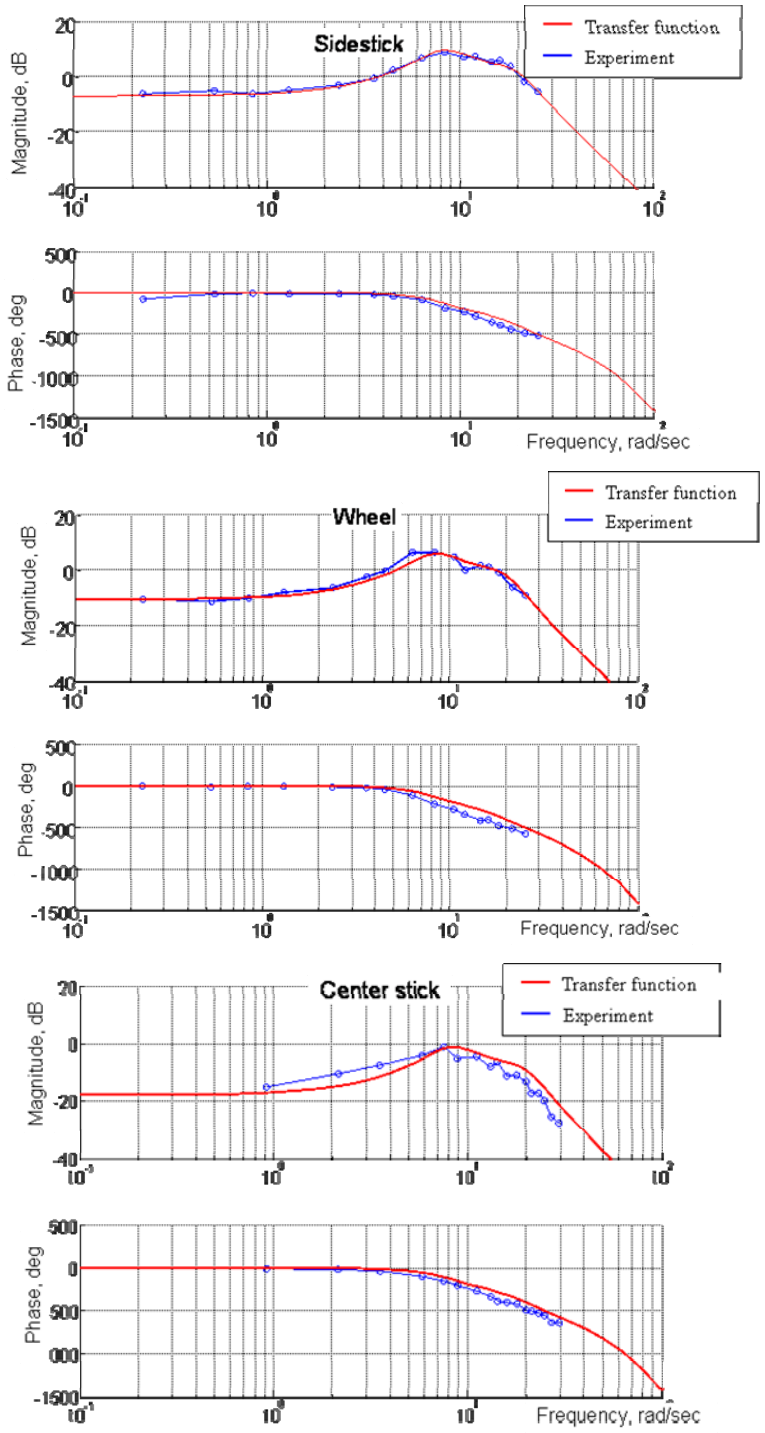

Figure 15: Active pilot. Comparison of the experimental describing function with that calculated in accordance with the identified transfer functions

3.2 Biodynamical pilot modelling

As for the active pilot, the structure of the transfer function for the biodynamical pilot model is selected from the point of view of the best coincidence of the calculated and experimental data.
The following transfer function structure provides the best agreement between the calculated and experimental describing functions:

$$Y_{bp}(s) = K \cdot \left(\frac{Ts+1}{T_I s+1} \right) \cdot \left[\frac{1}{T_1^2 s^2 + 2T_1\zeta_1 s + 1} \right] \cdot \left[\frac{1}{T_2^2 s^2 + 2T_2\zeta_2 s + 1} \right]. \qquad \textbf{(6)}$$

For the “zero” set of feel system characteristics, the values of the parameters in function (6) are as follows:

- for the sidestick: K=180mm/g, T=0.4s; T_I=1.0s; T_1=0.1s, ζ_1=0.45; T_2=0.05s; ζ_2=0.1;
- for the wheel: K=50mm/g, T=0.4s; T_I=3.0s; T_1=0.08s, ζ_1=0.2; T_2=0.05s; ζ_2=0.1.

If the feel system characteristics are non-zero, the parameters of function (6) change in accordance of the functions shown in Figure 16 for force gradient and in Figure 17 for damping.

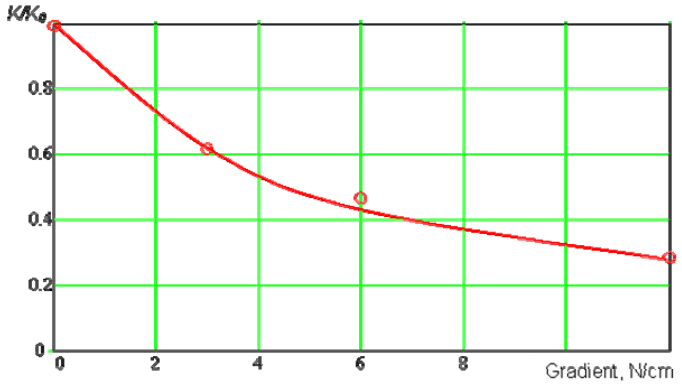

Figure 16: Biodynamical pilot. Transfer function parameter adjusting for the effect of inceptor force gradient

The increase of force gradient, i.e. limb-manipulator system stiffness, leads to biodynamic interaction reduction, which is expressed by gain K (Figure 16, K_0 is the value for “zero” gradient). The values of other parameters in (6) can be left unchanged, since their effect is negligible.
The inceptor damping leads to more complicated interdependence of the parameters of function (6), which is caused, seemingly, by more complex biomechanical interaction in the body-limb-manipulator system. To simplify the process of adjustment, two parameters were selected, which changes are more noticeable. They are: parameter T_I and the damping ratio of the second oscillatory unit ζ_2. Their adjustment functions are shown in Figure 17 (in the Figure the parameters are shown referred to their value for “zero” damping). As recent experiments showed, the regularities shown in Figure 17 for the effect of damping are true if the force gradient is of non-zero value (see Figure 21 for confirmation).

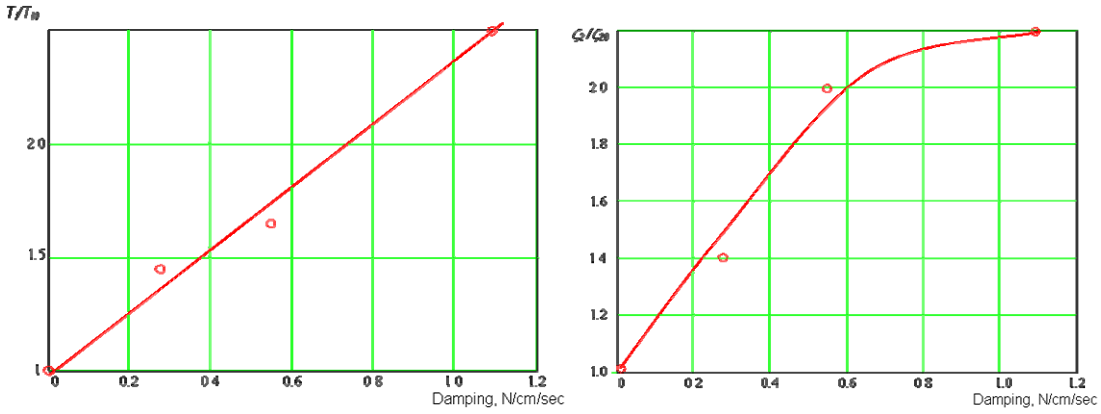

Figure 17: Biodynamical pilot. Transfer function parameter adjusting for the effect of inceptor damping

Figures 18 - 21 confirm the validity of the identified transfer functions by their comparison with the experimental describing functions of the biodynamical pilot models.

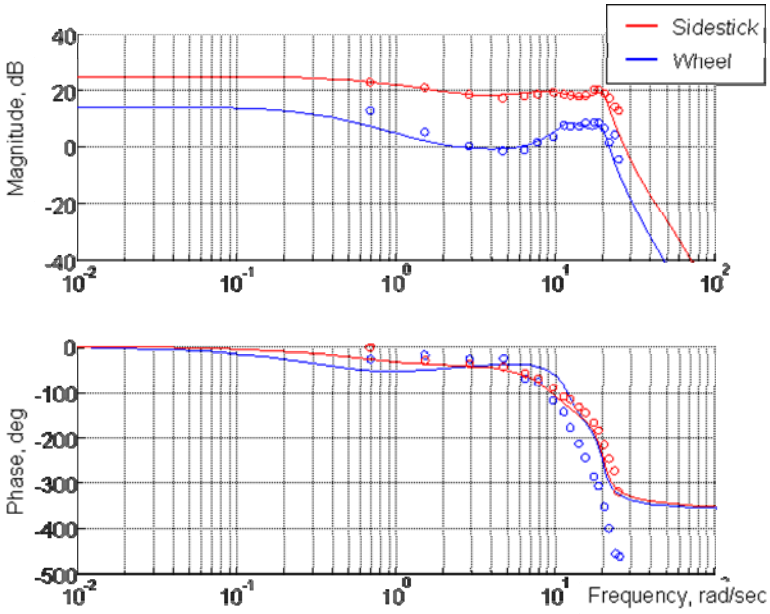

Figure 18: Biodynamical pilot. Comparison of the experimental describing function with that calculated in accordance with the transfer functions. Different inceptors

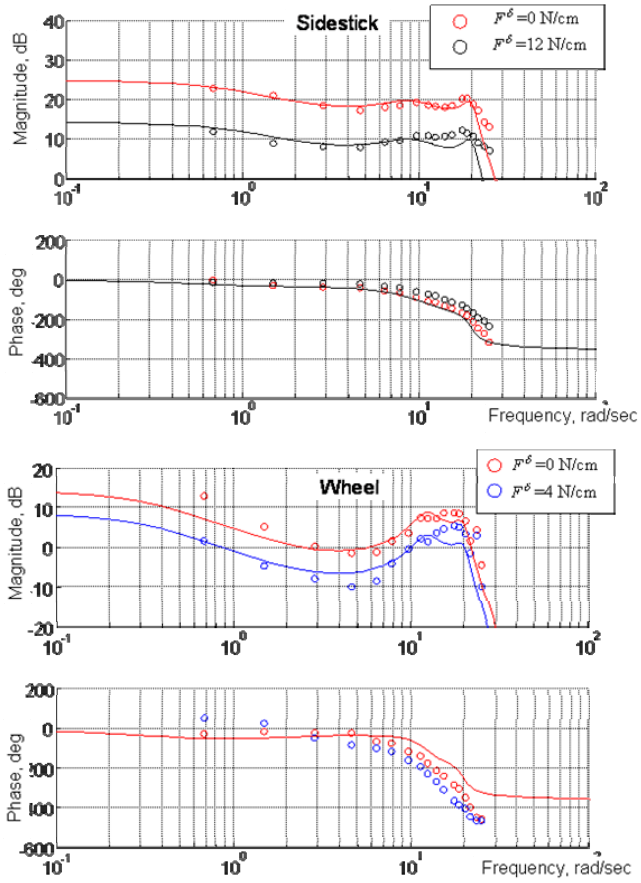

Figure 19: Biodynamical pilot. Comparison of the experimental describing function with that calculated in accordance with the transfer functions. Sidestick, wheel, - effect of force gradient

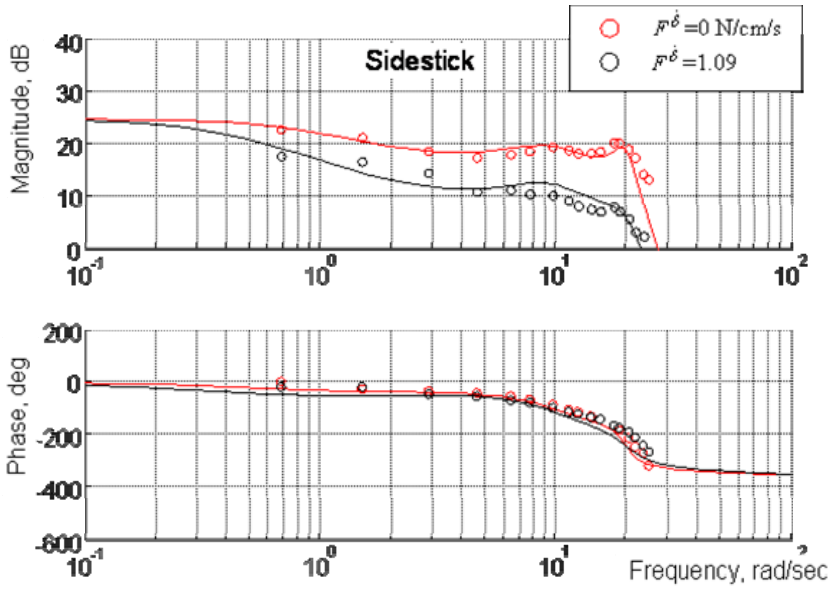

Figure 20: Biodynamical pilot. Comparison of the experimental describing function with that calculated in accordance with the transfer functions. Sidestick, effect of damping for “zero” force gradient

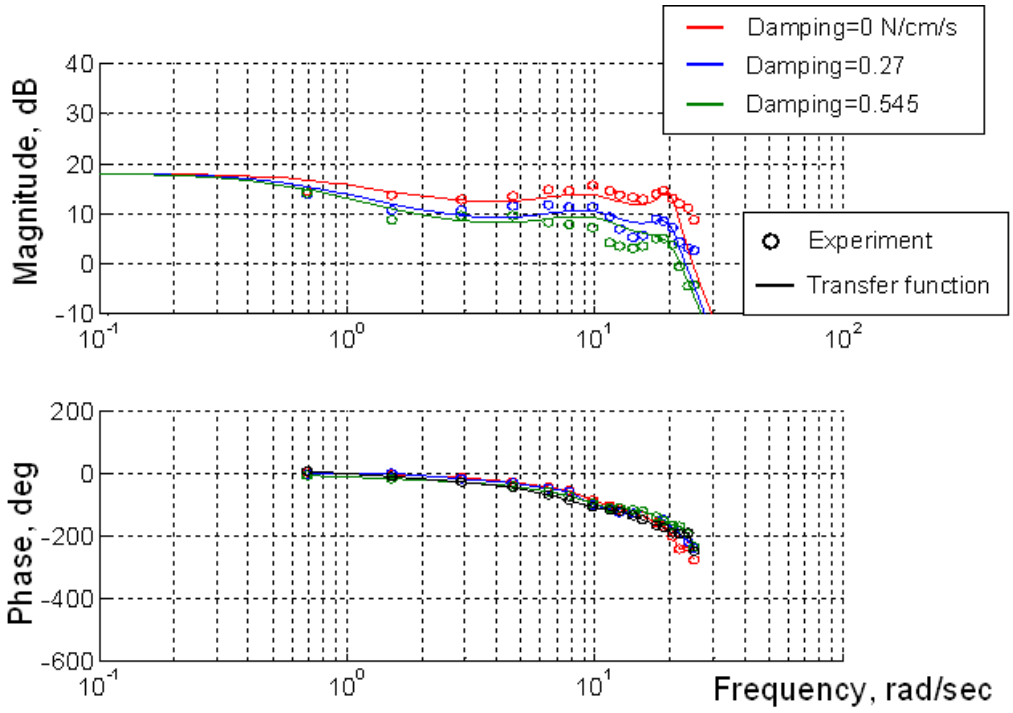

Figure 21: Biodynamical pilot. Comparison of the experimental describing function with that calculated in accordance with the transfer functions. Sidestick, effect of damping for “optimum” force gradient

4. Results and Conclusions

1. The idea is substantiated of the pilot activity splitted into “active pilot” visually controlling the aircraft, and “biodynamical pilot” describing involuntary inceptor displacements under high-frequency lateral accelerations.
2. Thorough analysis is conducted of the experimental describing functions received in the course of biodynamical experiments, which made the database for active and biodynamical pilot modelling. The analysis, in particular, showed the following:
   - Feel system characteristics do not affect active pilot model, but their deviation from the “optimum” values can cause handling qualities ratings deterioration.
   - Biodynamical interaction (biodynamical pilot model) depends on inceptor type: the smallest BDI is observed for the wheel.
   - Inceptor damping is the most effective method to suppress biodynamical interaction, since it considerably reduces the high-frequency inceptor oscillations, and, in the same time, does not cause pilot ratings deterioration in a wide range of its variation.
3. Transfer function identification is made for active and biodynamical pilot models. For the biodynamical pilot model, the rules of parameter adjustment are determined as a function of force gradient and damping.
4. The conducted analysis and the identified transfer functions will be used to develop criteria to assess the effect of aircraft structural elasticity with regard to inceptor feel system characteristics.

References

[1] L.Zaichik, V.Rodchenko, Y.Yashin, et.al. 1999. Acceleration perception. AIAA MST Conference. AIAA-99-4334. Portland OR.

[2] V.Rodchenko, L.Zaichik, Y.Yashin, I.Rufov, A.White. 2000. Theoretical approach to estimation of acceleration effects on piloting. AIAA MST Conference. AIAA-2000-4292. Denver CO.

[3] L.Zaichik, P.Desyatnik, K.Grinev, Y.Yashin. 2012. Effect of manipulator type and feel system characteristics on high-frequency biodynamic pilot-aircraft interaction. ICAS paper 285. ICAS 2012. Brisbane. Australia.

[4] V.Rodchenko, L.Zaichik, Y.Yashin, et.al. 1994. Investigation of controllability criteria of class III aircraft equipped with a sidestick. WL-TR-96-3079. Wright-Patterson Laboratory.

[5] V.Rodchenko, L.Zaichik, Y.Yashin. 1998. Similarity criteria for manipulator loading and control sensitivity characteristics. Journal of Guidance, Control and Dynamics. vol.21. No2: 307-314.